International Conference on Space Optics—ICSO 2008

Toulouse, France

14–17 October 2008

Edited by Josiane Costeraste, Errico Armandillo, and Nikos Karafolas

Coupled thermo-elastic and optical performance analyses of a reflective baffle for the BepiColombo laser altimeter (BELA) receiver

E. Heesel

T. Weigel

P. Lochmatter

E. Rugi Grond

International Conference on Space Optics — ICSO 2008, edited by Josiane Costeraste, Errico Armandillo, Nikos Karafolas, Proc. of SPIE Vol. 10566, 105661W · © 2008 ESA and CNES
CCC code: 0277-786X/17/$18 · doi: 10.1117/12.2308252

COUPLED THERMO-ELASTIC AND OPTICAL PERFORMANCE ANALYSES OF A REFLECTIVE BAFFLE FOR THE BEPI COLOMBO LASER ALTIMETER (BELA) RECEIVER

E. Heesel [(1)], T. Weigel [(1)], P. Lochmatter [(1)], E. Rugi Grond [(1)]

[(1)] Oerlikon Space AG, Schaffhauserstr.580, CH-8052 Zürich, SWITZERLAND, Email: eva.heesel@oerlikon.com

ABSTRACT

For the BepiColombo mission, the extreme thermal environment around Mercury requires good heat shields for the instruments. The BepiColombo Laser altimeter (BELA) Receiver will be equipped with a specular reflective baffle in order to limit the solar power impact. The design uses a Stavroudis geometry with alternating elliptical and hyperbolic vanes to reflect radiation at angles >38° back into space. The thermal loads on the baffle lead to deformations, and the resulting changes in the optical performance can be modeled by ray-tracing. Conventional interfaces, such as Zernike surface fitting, fail to provide a proper import of the mechanical distortions into optical models. We have studied alternative models such as free form surface representations and compared them to a simple modeling approach with straight segments. The performance merit is presented in terms of the power rejection ratio and the absence of specular stray-light.

1. INTRODUCTION

The BepiColombo Laser altimeter (BELA) has the objective to measure the surface topology of the planet Mercury.
The solar flux at Mercury Perihelion reaches 14,448 W m^{-2}, which is about 10 times that of the flux at the Earth. These high thermal loads require good heat protection of the instrument.
The Laser Altimeter Receiver will be equipped with a reflective baffle in order to limit the solar power impact. The interior surfaces of the baffle are specular reflective. The design uses a Stavroudis geometry [1] with alternating elliptical and hyperbolic vanes to reflect all incoming radiation at angles >38° back into space. The optical stray-light performance for the undeformed baffle has recently been assessed with forward and backward ray-tracing [2].
The baffle itself is exposed to heavy thermal loads leading to thermo-elastic distortions. The investigation of different geometry surfaces for modelling these distortions and their effect on the optical performance is subject of this paper.

2. MODEL GEOMETRY

The deformed baffle geometry was calculated with a finite element (FE) element model in NASTRAN, and the resulting specular stray-light performance was assessed by ray-tracing with the optical software ASAP.

Six elliptical and five hyperbolical segments are arranged in a Stavroudis geometry, whose focal points lie in the entrance plane of the baffle [3]. For the ideal undeformed baffle shape, all incoming radiation at angles >38° is reflected back into space. There is also a front ring for further thermal protection. The ring is included in the model, as it might be "seen" by reflected rays. A ray-trace for the baffle is shown in Fig. 1.

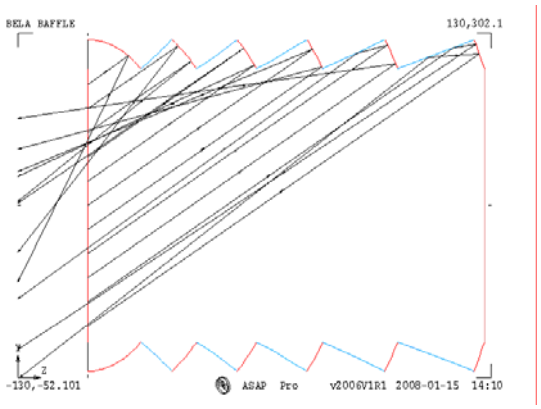

Fig. 1 BELA Receiver Baffle geometry

The original shape can be modeled by surfaces of revolution that are rotationally symmetric. The thermal loads of the solar radiation lead to structural deformation and hence loss of symmetry. A new surface geometry has to be found to model the deformed baffle shape and assess the optical performance.
The mechanical distortions in the thermo-elastic FE model have to be imported into the optical model. The distortions are both in axial and radial directions, which makes the use of polynomial functions difficult. Conventional interfaces, such as Zernike surface fitting, fail to provide a proper import of the mechanical distortions into optical models.
We have studied the baffle performance for geometry models with rational Bezier splines as free- form surface representations and compared them to a more simple modeling approach with straight segments.

3. STRAIGHT SEGMENT MODEL

The baffle geometry is modelled by rings in the radial direction that are connected by straight segments in the axial direction (along the optical axis).
The rings are divided into grid points (nodes) to generate a mesh that can be used in the FE model in NASTRAN and in the optical model in ASAP.

The geometry is defined, such that

- in the radial direction, there are 90 nodes per ring, separated by 4° from each other;
- in the axial direction, the nodes of a ring are connected by a straight line to the corresponding node that has the same angle on the neighbouring ring. Each baffle vane consists of 21 rings (20 segments);
- the front ring is modelled by 5 rings with different diameters.
- The total number of nodes is about 20 800, which are used to generate the mesh, shown in Fig. 2 for the finite element model.
- The thermo-elastic deformations in the FE model result in displacements of the nodes, which are applied to nodes of the original mesh in the optical model to obtain a deformed baffle shape.

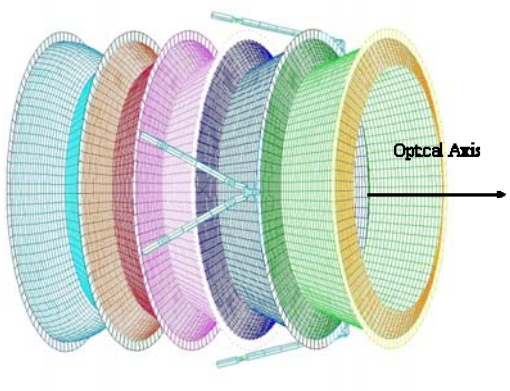

Fig. 2 BELA Receiver Baffle mesh generated in NASTRAN

4. FREE-FORM SURFACES

A model with parametric surfaces has been built from Rational Bezier Spline curves:

$$P(t) = \frac{(1-t)^2 w_0 P_0 + 2t(1-t)w_1 P_1 + t^2 w_2 P_2}{(1-t)^2 P_0 + 2t(1-t)P_1 + t^2 P_2} \quad (1)$$

The points P_0 and P_2 are the respective start point and the end point of a segment. When t runs from 0 to 1, $P(t)$ traces out a line segment between P_0 and P_2. The point P_1 is a control point which controls the shape of the curve between P_0 and P_2, and w is a weighting factor. An example is shown in Fig. 3.

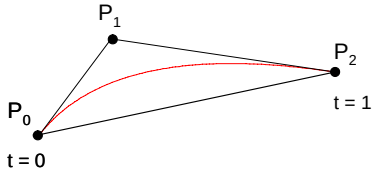

Fig. 3 P_0 and P_2 are connected by a Bezier spline curve (red), with P_1 as control point

Solving Eq. 1 for unknown P_1 and w is not simple. For the undeformed baffle shape, the P_1 and w can be calculated, using the tangents of the curve through P_0 and P_2.
In this case, P_1 usually lies close to the curve that connects P_0 and P_2. The displacements of P_0 and P_2 can be calculated in the FE model in the same way, as described in section 3. It was assumed that the displacement of P_1 is the same as that of a nearby point P_{11} that lies on the curve between P_0 and P_2 and which can therefore be incorporated in the FE mesh.

The following method was applied:

- Each hyperbolical/elliptical segment was divided into smaller segments, and the P_1 and w calculated in ASAP for the undeformed baffle shape
- The P_1 was used to calculate a nearby point P_{11} on the curve.
- The FE model calculated the displacements of P_0, P_2, and P_{11}, resulting in displacement vectors v_0, v_2, and v_{11}.
- The optical model used the following displacements for the new points:

  $P_0' = P_0 + v_0$;

  $P_2' = P_2 + v_2$;

  $P_1' = P_1 + v_{11}$;
- The weighting factor for P_1' was taken to be the same as for P_1.

The rings were divided into 180 nodes, separated by 2° from each other, and every second node was taken as control point P_1. As a results, the number of nodes doubled, leading to longer computing time. It should be noted that this aspect will set a limit to the total number of nodes in FE and optical models.

5. THERMO-ELASTIC ANALYSIS

The investigation of the thermo-elastic behaviour of the baffle was based on a NASTRAN FE model. The FE model only covers the major structural aspects. The rotationally symmetrical baffle body was meshed with thin shell elements (CQUAD4 and CTRIA3) while the three bipods were modelled with beam elements (CBEAM). The spatial resolution of the FE mesh was selected such that the model could be used to derive the optical performance of the baffle.
Thermal simulations delivered the selected temperature distributions across the nodes of the thermal baffle model. The thermal model, however, contains much less nodes than the mechanical model. Furthermore, the nodes of the two models do no coincide. Thus, the temperatures at the nodes of the mechanical baffle model were calculated by interpolation based on the temperatures given at the thermal nodes.

This included a two-dimensional interpolation based on the two major coordinates, i.e. the axial and the circumferential axes, with the shell structure of the baffle body. With the beam structures of the bipods the temperature development along the beam axis was interpolated.
For the thermo-elastic calculations of the baffle in NASTRAN each bipod leg was clamped.
The thermo-elastic analysis showed a non-axisymmetric deformation of the baffle under the influence of the sun radiation. The resulting stress distribution proved the isostatic suspension of the baffle body by the bipods.

6. RESULTS

The baffle geometry was tested for several different thermal load cases. Here, we present the following two representative cases.

A) Maximum gradients in the first elliptical segment; intermediate angle of incidence.

B) Maximum temperature in baffle; high angle of incidence.

The angle of incidence is important for assessing the accuracy of the baffle geometry, as more rays have to be reflected by the first elliptical segment with increasing angle of incidence.
The performance figure of merit is the fraction of rays that reach the rear of the baffle as specular stray-light; expressed in promille.
The ray-tracing was performed with the following parameters:

- Nominal angle of incidence of solar rays: calculated in thermal model from the orbit;
- Direction of incidence: calculated from the highest temperature point in the finite element model.

The simplified baffle geometry in the optical model leads to an inaccuracy in the ray-tracing. The following measures were taken to analyse the sensitivity and average over the stray-light performance resulting from the simplified baffle geometry.

- The angle of incidence was varied by about ± 5° with respect to the nominal angle of incidence;
- The ray-tracing was performed with six different numbers of rays, such that the baffle surface was "sampled" with different densities of rays, and the average taken of the six performance values.
- The analyses were repeated for the same parameters with the undeformed baffle for comparison.

For the ideal baffle geometry, all incident rays at angles >38° are reflected back into space, such that there is no specular stray-light. For the approximated geometries, there was stray-light for the undeformed shape, which represented an initial uncertainty.

In some cases, the amount of stray-light of the deformed baffle was less than that of the undeformed baffle. We attribute this to the initial uncertainty in the geometry as well as to the possibility of an improved performance for a deformed baffle; i.e. the deformed baffle shape might be a better approximation to the ideal geometry than the undeformed shape.

A) Intermediate angle of incidence: 50°, 55°, 60°

Fig. 4 shows the temperature distribution on the deformed baffle. The highest temperature (red) is 128°C.

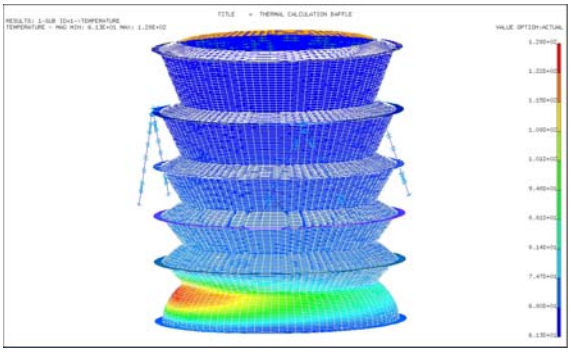

Fig. 4 Temperature distribution on BELA Receiver Baffle mesh

Straight Segment Model
Table 1 shows the stray-light performance for the undeformed and deformed baffle for six different numbers of rays.

Table 1 Baffle performance for 50°, 55°, 60° angle of incidence- straight segments

Angle of incidence	50°		55°		60°	
	Undeformed	Hot case 1 t = 7040 s	Undeformed	Hot case 1 t = 7040 s	Undeformed	Hot case 1 t = 7040 s
Number of rays	Stray-light Promille	Stray-light Promille	Stray-light Promille	Stray-light Promille	Stray-light Promille	Stray-light Promille
10029	0.4	0.1	0.4	0.3	0.8	0.5
17905	0.4	0.6	0.6	0.3	0.7	0.8
31757	0.4	0.3	0.7	0.5	1.1	0.5
96765	0.6	0.5	0.4	0.4	1.0	0.6
197157	0.6	0.6	0.7	0.5	1.0	0.6
491441	0.6	0.5	0.6	0.5	1.0	0.5
Average	0.5	0.4	0.6	0.4	0.9	0.6

The average amount of specular stray-light is less than 1 Promille for the undeformed baffle for all angles of incidence. The deformed baffle shows similar performance, with lower average. The performance of the deformed baffle should be compared relative to that of the undeformed baffle, as the model introduces an inaccuracy in the geometry.

Bezier splines model
Table 2 shows the stray-light performance for the undeformed and deformed baffle for six different numbers of rays.

Table 2 Baffle performance for 50°, 55°, 60° angle of incidence- Bezier splines

Angle of incidence	50°		55°		60°	
	Undeformed	Hot case 1 t = 7040 s	Undeformed	Hot case 1 t = 7040 s	Undeformed	Hot case 1 t = 7040 s
Number of rays	Stray-light	Stray-light	Stray-light	Stray-light	Stray-light	Stray-light
	Promille	Promille	Promille	Promille	Promille	Promille
10029	3.1	1.6	1.1	2.6	1.4	1.5
17905	1.7	1.6	1.5	1.5	1.7	1.3
31757	1.9	1.4	2.2	2.0	1.7	1.9
96765	2	1.4	1.7	1.9	2.0	1.4
197157	1.9	1.2	1.9	1.9	1.9	1.4
491441	2	1.4	1.8	1.9	1.9	1.4
Average	2.1	1.4	1.7	2.0	1.8	1.5

The average amount of stray-light is up to 2.1 Promille for the undeformed baffle. The stray-light performance of the deformed baffle relative to the undeformed baffle is less than 1 Promille. The overall performance is worse than in the straight segment model.

B) High angle of incidence: 70°, 75°, 80°, 85°

Fig. 5 shows the temperature distribution on the deformed baffle. The highest temperature (red) is 126°C.

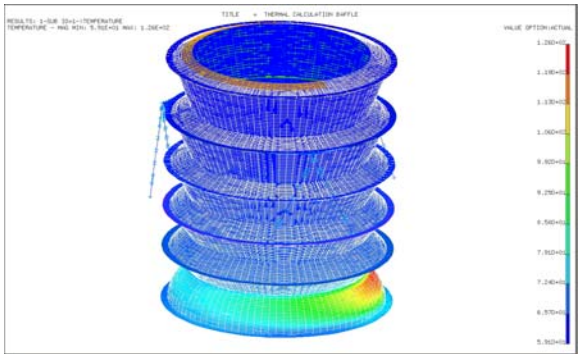

Fig. 5 Temperature distribution on BELA Receiver Baffle mesh

Straight Segment Model

Table 3 shows the stray-light performance for the undeformed and deformed baffle.

Table 3 Baffle performance for 70°, 75°, 80°, 85° angle of incidence- straight segments

Angle of incidence	70°		75°	
	Undeformed	Hot case 3 t = 2000 sec	Undeformed	Hot case 3 t = 2000 sec
Number of rays	Stray-light	Stray-light	Stray-light	Stray-light
	Promille	Promille	Promille	Promille
10029	2.4	1.2	1.3	2.5
17905	1.4	0.9	1.0	2.7
31757	1.7	1.1	1.4	2.7
96765	1.9	1.0	1.7	2.3
197157	1.9	1.0	1.6	2.2
491441	1.8	1.0	1.5	2.3
Average	1.9	1.0	1.4	2.5

Angle of incidence	80°		85°	
	Undeformed	Hot case 3 t = 2000 sec	Undeformed	Hot case 3 t = 2000 sec
Number of rays	Stray-light	Stray-light	Stray-light	Stray-light
	Promille	Promille	Promille	Promille
10029	23.4	24.1	16.4	15.4
17905	23.0	23.8	18.3	17.2
31757	22.4	24.7	19.1	17.8
96765	23.3	24.5	19.2	17.6
197157	22.9	23.9	19.1	17.5
491441	23.3	24.1	18.8	17.3
Average	23.1	24.2	18.5	17.1

The average amount of stray-light for the undeformed baffle is 1.9 Promille for 70°, while it is 23.1 Promille for 80°. This trend shows that the amount of stray-light become greater for higher angles of incidence. The stray-light at 85° is less than that at 80°; we contribute this behaviour to the inaccuracy of the model. The stray-light amount for the deformed baffle relative to the undeformed baffle is within 1.4 Promille.

Bezier splines model

Table 4 shows the stray-light performance for the undeformed and deformed baffle.

Table 4 Baffle performance for 70°, 75°, 80°, 85° angle of incidence- Bezier splines

Angle of incidence	70°		75°	
	Undeformed	Hot case 3 t = 2000 sec	Undeformed	Hot case 3 t = 2000 sec
Number of rays	Stray-light	Stray-light	Stray-light	Stray-light
	Promille	Promille	Promille	Promille
10029	0.9	0.7	1.8	3.8
17905	1.3	0.6	2.5	4.3
31757	1.8	0.6	2.3	5.3
96765	1.9	0.7	1.6	4.2
197157	1.6	0.7	2.1	4.4
491441	1.7	0.8	1.9	4.3
Average	1.5	0.7	2.0	4.4

Angle of incidence	80°		85°	
	Undeformed	Hot case 3 t = 2000 sec	Undeformed	Hot case 3 t = 2000 sec
Number of rays	Stray-light	Stray-light	Stray-light	Stray-light
	Promille	Promille	Promille	Promille
10029	5.9	9.7	4.5	4.1
17905	5.5	9.7	5.0	5.6
31757	5.6	10.0	4.8	5.6
96765	5.8	9.7	4.8	5.3
197157	5.7	9.7	4.6	5.3
491441	5.7	9.8	4.7	5.3
Average	5.7	9.8	4.7	5.2

For 70°, the performance is slightly better than in the straight segment model, while for 75° it is worse. For the higher angles, the average amount of stray-light is up to 6 Promille for the undeformed baffle and up to 10 Promille for the deformed shape, which is much lower than in the straight segment model.

7. CONCLUSION

A) Intermediate angles of incidence

In the straight segment model, the stray-light in the undeformed baffle represents an initial uncertainty of up to ~1 Promille. The stray-light for the deformed baffle relative to the undeformed baffle is within 1 Promille. Therefore, the performance of the deformed baffle is within the uncertainty of the model.
In the Bezier splines model, the average stray-light amount is up to 2.1 Promille for the undeformed baffle. The stray-light of the deformed baffle relative to the undeformed baffle is less than 1 Promille. The overall performance is worse than in the straight segment model.

B) High angles of incidence

In the straight segment model, the stray-light amount in the undeformed baffle is up to ~23 Promille. This reflects the problem with the modelling accuracy at high angles of incidence, as more rays are reflected by the first elliptical segment. The stray-light for the deformed baffle relative to the undeformed baffle is within 1.4 Promille, which is slightly greater than the performance at intermediate angles of incidence.
In the Bezier splines model, the performance is better than in the straight segment model for most angles of incidence. The improvement is very good for 80° and 85°, which suggests a better representation of the geometry by Bezier splines than by straight segments for high angles of incidence. However, at 75°, the performance is worse than in the straight segment model, such that the result is not general.

General conclusions

The investigation showed that while the Bezier splines method can work better than the linear one for selected cases, it is not easy to control the parameters, such that the results are always more accurate than the simplified geometry with straight segments.
The comparison of the straight segment model with the Bezier splines showed that the average performance of the former is better for medium angles of incidence, while the Bezier splines seem to give a more accurate representation for higher angles of incidence.
In order to improve the stray-light performance in the modelling, a more complex non-linear fitting of the baffle shape would be necessary. A promising method could be NURBS (non-uniform rational Bezier splines), as they have two control parameters to map the surface in three-dimensional space. NURBS are not implemented in all software applications, such that additional tools and interfaces might be necessary for a successful transfer from the FE model data into an optical model.

In the method presented here, the Bezier splines have uncertainties in the control of the parameters for the deformed case, such that we prefer the results of the approximation with straight segments, even if it has a "birth" error. The straight segment approximation gives remarkably good performance results, whilst keeping the computing efforts reasonable.

ACKNOWLEDGEMENT

The work presented herein was performed in the frame of BELA Phase B2 and funded by the Swiss Space Office. We would like to thank ESA and the BELA Team from the University of Bern for supporting this activity.

9. REFERENCES

[1] O.N. Stavroudis, L.D. Foo; "System of reflective telescope baffles", *Optical Engineering*, Vol 33 No 3 p.675-680

[2] T. Weigel, E. Rugi-Grond, K. Kudielka; "Straylight Analysis of the BepiColombo Laser Altimeter", *Proc. 'SPIE Europe Optical Systems Design', Glasgow, United Kingdom, 2-5 September 2008 (SPIE 7100A-50)*

[3] E. Rugi-Grond, T.Weigel, A. Herren, M. Dominguez Calvo, U. Krähenbühl, D. Mouricaud, H. Vayssade; "Reflective Baffle for BEPICOLOMBO Mission", *Proc. '6th Internat. Conf. on Space Optics', ESTEC, Noordwijk, The Netherlands, 27-30 June 2006 (ESA SP-621, June 2006)*